D 50128
ADVENGMAT
ISSN 1438-1656
Vol. 9 – No. 3
March, 2007

ADVANCED ENGINEERING MATERIALS

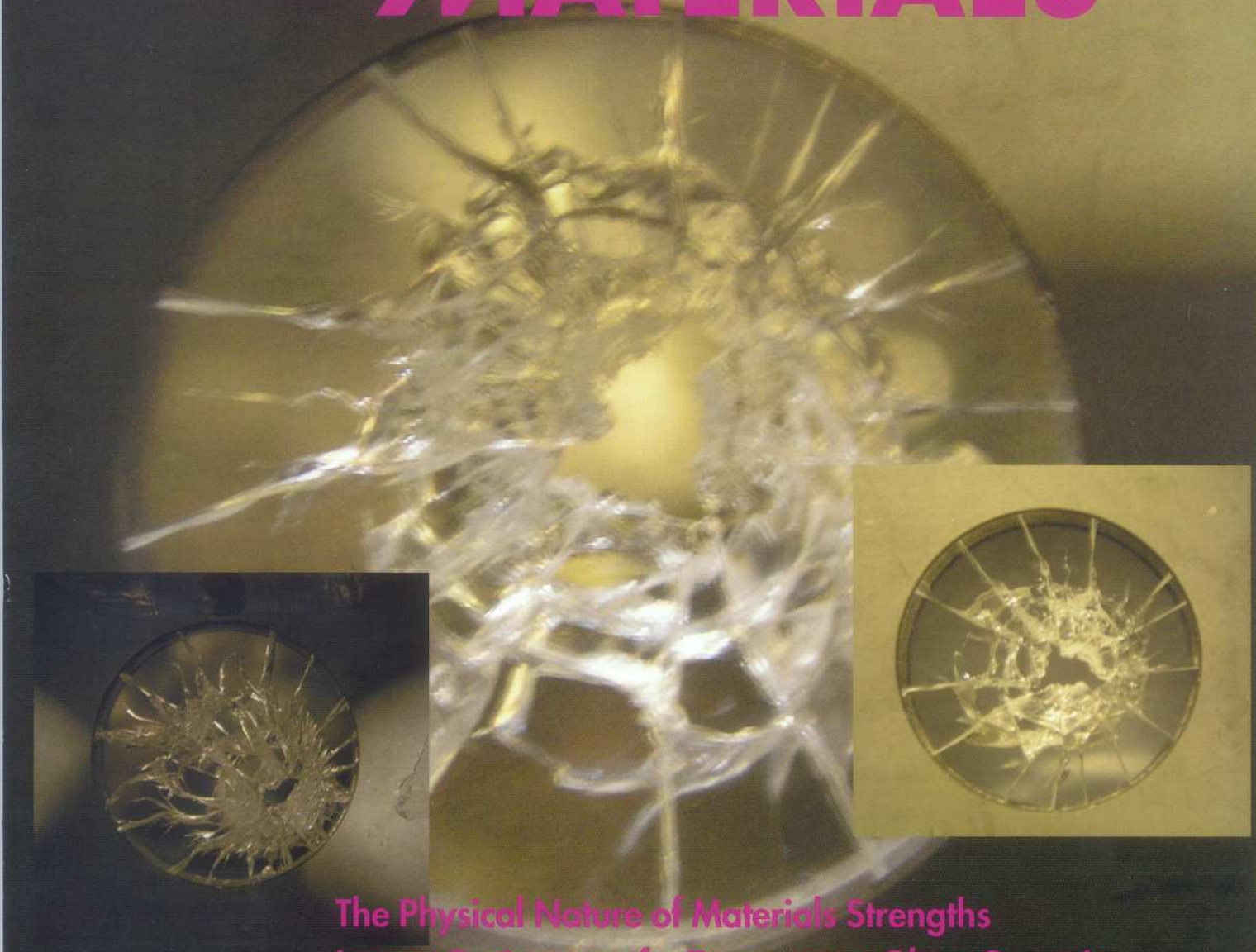

The Physical Nature of Materials Strengths
Impact Resistance of a Transparent Glass-Ceramic
Deformation and Fracture of a Hollow Bulk-Metallic Glass
Crystalline Silicon Solar Cell Development

WILEY-VCH

DGM SF2M SVMT

BICENTENNIAL 1807 WILEY 2007 BICENTENNIAL

DOI: 10.1002/adem.200600237

Mechanical Properties and Impact Resistance of a New Transparent Glass-Ceramic**

By *Thiana Berthier da Cunha, Jeremy P. Wu, Oscar Peitl, Vladimir M. Fokin, Edgar D. Zanotto, Lorenzo Iannucci, Aldo R. Boccaccini**

The focus in ceramic armour development today is towards improved protection capability combined with an overall reduction in production cost.[1–5]

Because of their brittle nature, ceramics and glasses are susceptible to localized surface damage in the form of cracking when subjected to impact by foreign objects.[6,7] Much work has been carried out on the dynamic impact behaviour of ceramics and glasses.[1–5] Tests have been carried out using small ceramic or metallic spheres, impacting at high speed in so-called ballistic tests. In these tests, projectiles are accelerated toward their target by utilizing specialised devices called gas guns.[8–14]

The development of transparent glass-ceramics with a reinforced surface layer is a promising approach to novel armour materials since glass-ceramics combine high strength with improved fracture toughness compared with glass and yet they can be reliably produced using cost-effective processing methods.[15,16] A number of technical reports have been published in the last forty years regarding different types of transparent glass-ceramics,[17–20] but very few focused on their use as armour materials. The most attractive advantage of glass-ceramics is the possibility of using standard glass processing methods followed by controlled heat treatment, which is a fast and reliable production method, resulting in almost no residual porosity in the materials. Moreover the melting plus heat-treatment route offers very good reproducibility compared with the alternative method based on powder processing and sintering commonly used in polycrystalline ceramics, which is prone to microstructure inhomogeneity. In the majority of previous investigations, transparent glass-ceramics have been obtained, which exhibit the presence of nanocrystals within an amorphous matrix.[21,22] This nanostructure (with less than 70 % crystalline phase) guarantees optical transparency since the crystal size is smaller than the wavelength of visible light. The two principal conditions for achieving high transparency are low optical scattering and low atomic absorption in the visible range.[23–25]

Transparent glass-ceramics appear to be an ideal material for advanced armour applications due to their relatively good transparency, low density, relatively high fracture strength as well as their thermal and chemical stability. However, compared with the most popular polycrystalline ceramics (e.g. Al_2O_3), glass-ceramics exhibit lower fracture toughness.[26–30]

The fracture toughness of glass-ceramics can be increased by using the ion-exchange method, similarly to that used in chemically toughened glass. The technique of ion-exchange is one of the most effective alternatives to minimize the detrimental effect of surface flaws in glass bodies (inherent to their processing and use) because it produces compressive stresses on the glass surfaces by substituting the smaller ions (e.g. Na^+) in the glass by larger ions (K^+), a component of a molten salt bath (KNO_3). Strengthened glass therefore requires higher stresses for catastrophic crack initiation.[31–35]

The purpose of the present work was to analyse the impact resistance of a new type of transparent glass-ceramic, which has been recently developed.[36] It is a completely new material having up to 96 % crystallinity with crystal size of the order of microns (instead of nanometric) and still transparent in the visible range. The focus of this study was on investigating crack propagation behaviour under quasi-static conditions and on the macroscopic response under impact ballistic impact loading. Mechanical properties such as Young's modulus, hardness, and fracture toughness were also determined. The materials response under impact loads was studied within the low-velocity regime using a laboratory gas gun.

[*] *T. Berthier da Cunha, Dr. O. Peitl, Dr. V. M. Fokin, Prof. E. D. Zanotto*
Vitreous Materials Laboratory
Dept. Materials Engineering
Federal University of São Carlos, Brazil
E-mail: www.lamav.ufscar.br
Dr. habil. A. R. Boccaccini, Dr. J. P. Wu
Department of Materials
Imperial College London
London SW7 2BP, UK
E-mail: a.boccaccini@imperial.ac.uk
Dr. L. Iannucci
Department of Aeronautics
Imperial College London
London SW7 2AZ, UK

[**] *The research was partially funded from grants of ADEMAT (European Union) and Capes (Brasil) . Part of the experimental work was performed in the Aeronautics Department at Imperial College London, acknowledgements to Joseph Meggyesi for experimental assistance.*

COMMUNICATIONS

The material investigated was a glass-ceramic formed by a soda-lime-silica glass matrix containing homogeneously distributed crystals (5–10 μm) and no porosity.[36] The crystals are complex solid solutions containing all the elements of the parent glass ($Na_{4+2x}\ Ca_{4-x}\ Si_6\ O_{18}$; $0 < x < 1$). The typical microstructure of the glass-ceramic with 96-97 vol.% crystalline phase is shown in Figure 1 (crystallinity values are quoted in vol. % throughout the paper). Cubic shaped crystals can be observed homogenously distributed and the crystal size appears to be > 10 μm. The same crystalline morphology was observed in all other samples. The optical transmittance of a glass-ceramic sample (4 mm thick, 96 vol.% crystalline) is shown in Figure 2 in comparison with that of window glass. The transparency in the present glass-ceramics, which contain relatively large crystals (micron-sized), is due to the low optical scattering achieved in the microstructure. Despite their relatively large grain size (um), the materials are transparent to visible light because, with heat treatment, both the residual glass phase and crystals undergo continuous compositional changes in such way that the refractive index of the residual glass is always almost the same as that of the crystals, i.e. they differ by only 0.015. [36]

A plot of the Young's modulus as a function of crystalline fraction is presented in Figure 3(a). The elastic modulus of the glass (80 GPa) is lower than the value of the glass-ceramic (124 GPa), as expected. An increase in elastic modulus after crystallization is observed, but there is no dependence of elastic modulus on the ion exchange toughening (IET) process, the values before and after ion exchange being remarkably similar (within the experimental error, which was 5 % in these measurements).

Hardness and indentation fracture toughness (IFT) were measured by the Vickers indentation method.[37,38] A plot of hardness as a function of crystalline fraction is presented in Figure 3(b). A slight increase in the value of hardness due to crystallization can be observed. The results show that the hardness values of the glass-ceramics do not depend on the IET treatment; in the glass sample, however, the hardness values strongly increased with IET treatment.

According to literature,[1,13] it is generally accepted that high hardness is necessary for good ballistic performance. It has been suggested; however, that improved ballistic performance may be achieved if an increase in toughness can be obtained without changing the yield stress of the material.[7,8] It is therefore important to consider the fracture toughness (K_{Ic}) as well as hardness in order to understand and identify the factors which must be optimised to improve the ballistic resistance of brittle materials. A plot of fracture toughness as function of crystalline fraction for the glass-ceramic tested in this investigation is shown in Figure 4. It can be seen that

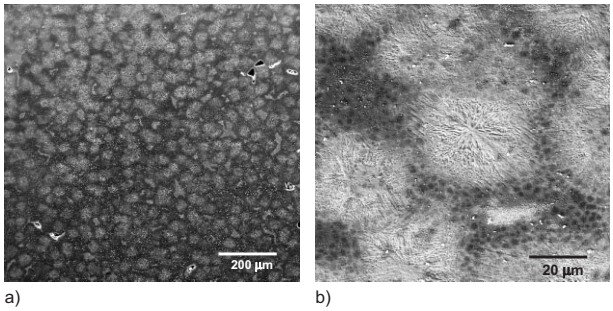

Fig. 1. SEM micrographs showing the typical microstructure of the glass-ceramic investigated (96 vol.% crystallized) with cubic crystals (crystal size > 10 μm) at a) low, b) high magnification.

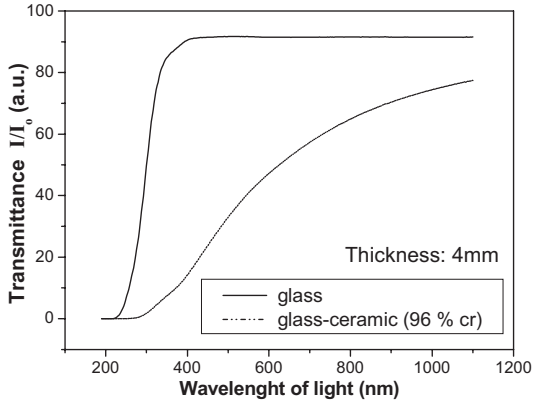

Fig. 2. Optical transmittance spectrum of a glass-ceramic sample (4 mm thickness, 96 vol% crystalline) and of window glass as a function of light wavelength.

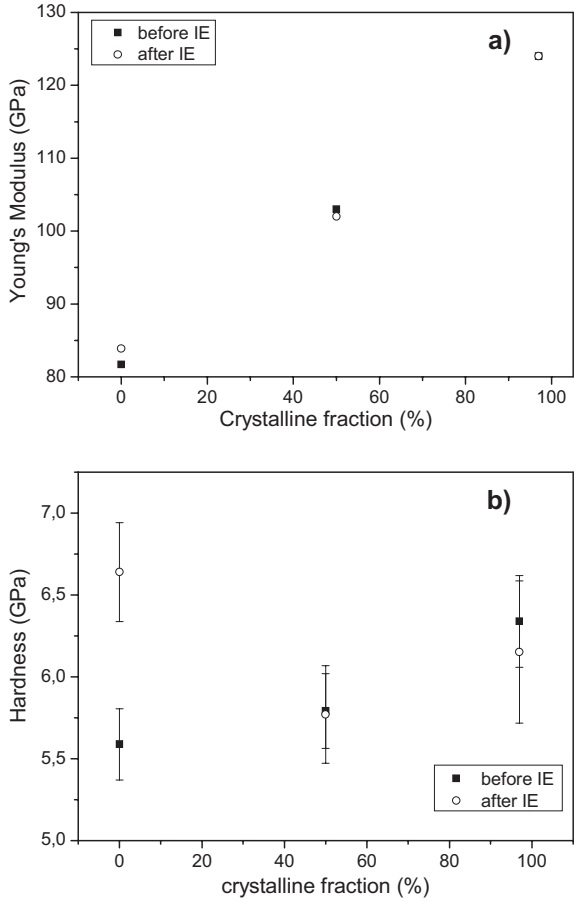

Fig. 3. Graphs showing (a) elastic modulus and (b) hardness of glass and glass-ceramics investigated, before and after IET treatment, as a function of crystalline fraction.

ADVANCED ENGINEERING MATERIALS

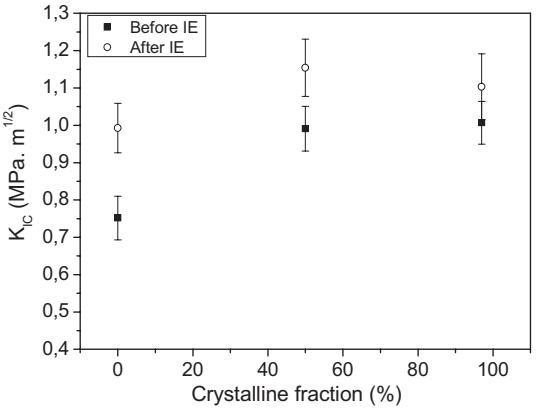

Fig. 4. Graph showing fracture toughness data, using indentation technique, as function of the crystalline fraction in transparent glass-ceramics.

the IET treatment tends to increase the fracture toughness in both the amorphous glass and the glass-ceramic samples. The macroscopically observed increase of fracture toughness with IET treatment is certainly due to the compressive stresses on the specimen's surface.[15] It must be noted, however, that surface compression stresses induced by IET treatment decrease with the distance from the surface. It is also evident that increase of crystallisation beyond 50 % does not lead to improvement of K_{IC}. We hypothesised that ion exchange can also occur within the Na-rich crystalline phase and this is why the technique was applied to this special type of highly crystalline glass-ceramic. As found in other systems,[39] ion exchange seems to occur also within the crystalline phase, which explains the observed increase in fracture toughness.

A typical indent on the surface of a glass sample is seen in (Fig. 5(a) while Fig. 5(b)) shows an indent on a glass-ceramic containing 96 % crystalline phase. Both samples were tested after IET treatment. One observes that crack propagation from each corner of the indent in both the glass and the glass-ceramic samples leads to a suitable crack pattern for indentation fracture toughness determination.[38] It can also be observed that cracks propagate in transgranular manner in the glass-ceramic, i.e. with a small deflection along the interface between crystals and matrix. One can speculate that 50 % is the optimal crystalline fraction to increase toughness in the present samples because of the residual stress field that exists around each crystal, which is favourable for crack deflection. When that crystallized fraction is exceeded, the residual stresses around each crystal start to overlap so that spontaneous microcracking might occur. Although it is difficult to observe this phenomenon for relatively small volume fractions of crystallized material, spontaneous cracking could be easily seen in our specimens, even with the naked eye, for the highest crystalline volume fractions.

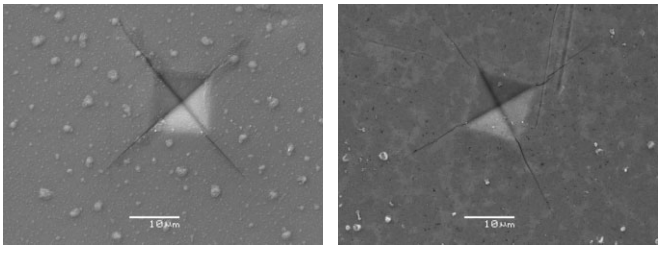

Fig. 5. SEM image of Vickers hardness indentations in samples after IET treatment: a) glass and b) glass-ceramic (96 vol.% crystallized).

Digital camera images showing the typical macroscopic damage after ballistic test at low impact energy using glass beads and impact velocity of approximately 80 m/s are presented in Figures 6(a–f) for the different samples investigated. Based on images of impacted samples, a methodology was developed in order to quantify the damage introduced in the samples as a consequence of ballistic loading. Visual inspection of samples led to the conclusion that microstructural damage is a combination of both macroscopic damage, for example in the form of perforation or total destruction of the sample, and microscopic damage, characterised by microcracking development, not necessarily leading to sample destruction. The extent of microcracking damage was determined by measuring the number of cracks. Numerical values between 1 and 3 were assigned to each damage condition found in impacted samples, as shown in Table 1. The overall damage parameter for each sample was then calculated by multiplying a factor related to macroscopic damage (second

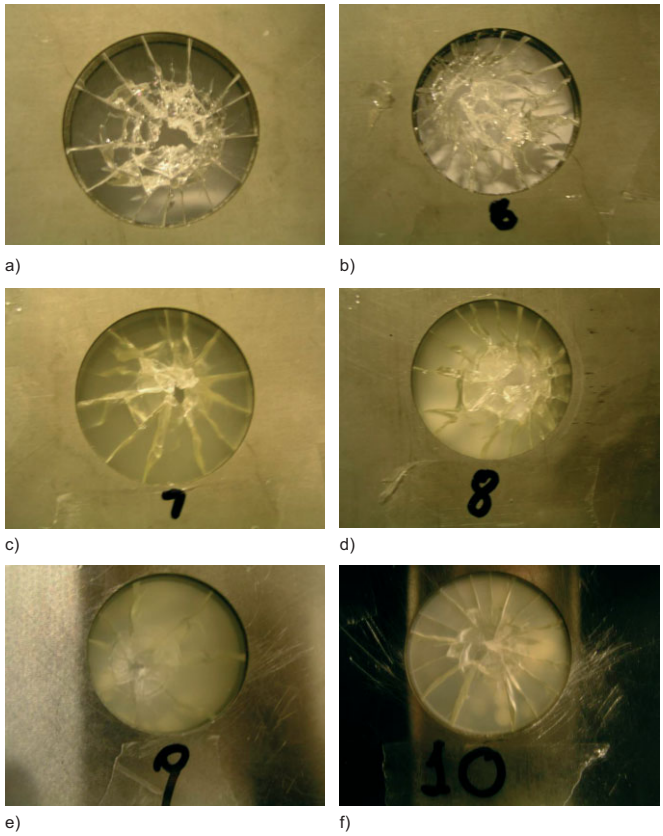

Fig. 6. Digital camera images showing the macroscopic damage after ballistic test at low impact energy (glass beads used as projectiles and velocity of 80 m/s) (a) glass, (b) glass after ion exchange, (c) glass-ceramic 50 % crystallized, (d) glass-ceramic 50 % cr. after ion exchange, e) glass ceramic 96 % crystallized (f) glass-ceramic 96 % cr. after ion exchange

Table 1. Factors assigned for quantification of damage as result of the ballistic tests performed on glass and glass-ceramic samples. The overall damage parameter is calculated for each sample by multiplying a factor related to macroscopic damage (second column) by a factor related to microcracking damage (fourth column) and used in Figs. 7a) and 7b) to plot damage maps for the materials investigated.

Quantification of Damage			
No perforation	1	Minimum microcracking	1
Perforation	2	Some microcracking	2
Destroyed	3	Maximum microcracking	3

column in Tab. 1) by a factor related to microcracking damage (fourth column in Tab. 1). The resultant numerical value, as a quantification of the damage suffered by the sample, was then used to plot damage maps for the materials investigated.

The results are shown in Figure 7(a) in the form of damage *versus* brittleness index multiplied by impact energy and in Figure 7(b) in the form of damage *versus* K_{IC} multiplied by impact energy. From values of H and K_{IC} the brittleness index B[40] was calculated by the following equation:

$$B = \frac{H}{K_{IC}} \quad (1)$$

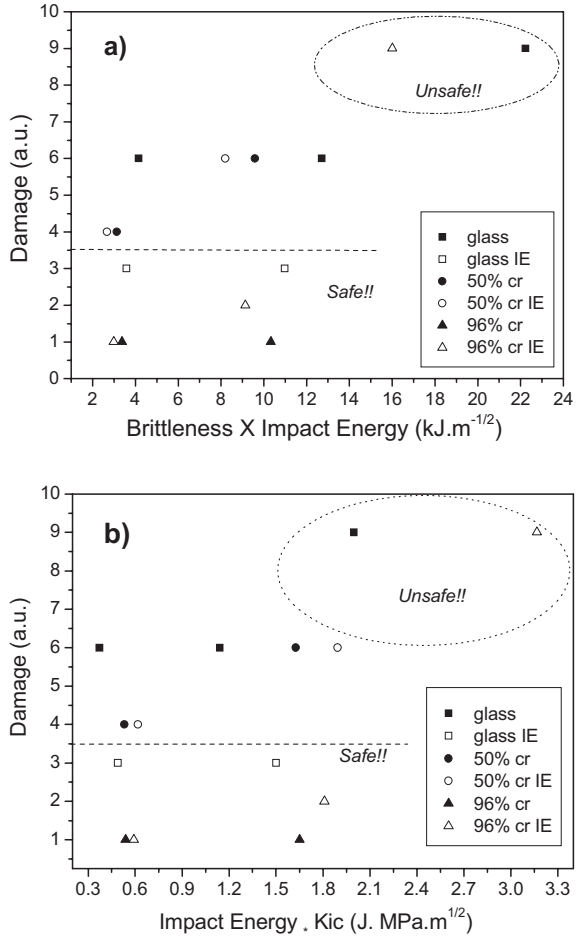

Fig. 7. Damage maps plotted using the damage parameters introduced in Table 1 as function of: (a) brittleness index X impact energy and (b) K_{IC} X impact energy. The glass-ceramics under investigation did not suffer penetration of the projectile in the safe region of the graph, even after having been substantially damaged by the impact of projectiles.

For the present work, three different impact energies were tested: 3 J, 2 J and 0.5 J. It is worthwhile noticing that the projectiles had different hardness which could lead to a different damage in the targets upon impact. However the parameter considered here as being the most critical affecting glass-ceramic damage was the impact energy as discussed next. The "unsafe" region shown in the graphs (Fig. 7) represents samples completely destroyed after ballistic impact, while the "safe" region represents samples which were not penetrated by the projectile, the word "penetration" is used here to refer to the cases when the projectile entered the specimen at the impact site emerging at the rear end of it. Samples with 96 % of crystallized fraction (with and without IET treatment) showed the lowest damage under ballistic impact. Despite the fact that they possess the largest fracture toughness values, samples with a 50 % of crystallized fraction did not show the best behaviour under impact, implying that fracture toughness is not the only parameter to be considered to assess ballistic impact resistance.

The brittleness index B, defined as the ratio between hardness and fracture toughness as proposed in the literature,[40] reflects the relative response of the material to deformation and fracture. In Figure 7(a), it is seen that the brittleness index allows the ordering of the materials according to their damage. Except for the glass sample after IET treatment, the hardness of all materials was similar (Fig. 3(b)), there is, therefore, no major difference between the damage maps in Figures 7(a) and 7(b). It can be concluded that hardness alone does not have a strong influence on the ballistic resistance of the present set of materials. The exception in this case was the glass sample after IET treatment which exhibited the highest hardness. The favourable combination of hardness and fracture toughness in this sample may explain why penetration of the projectile into this sample did not occur. The sample behaved 'safely' for all tested impact energies.

Figure 8 shows a general summary of the results obtained for indentation fracture toughness and hardness of all samples investigated. In this graph, the 96 % crystallised glass-ceramics and the IET treated glass, marked inside the dashed circle, showed the best impact resistance of all samples.

Summarising, the ballistic test technique was used to determine the impact resistance behaviour of glasses and glass-ceramics designed for use as transparent armours. The glass-ceramic containing a 96 % crystallized fraction, with and without IET treatment, did not suffer penetration by the glass or metallic spherical projectiles when subjected to ballistic impact loading at energies of up to 2 J. This was also the case for glass samples after IET treatment. This behaviour is the result of a favourable combination of hardness and fracture toughness. For the conditions of the present tests, pene-

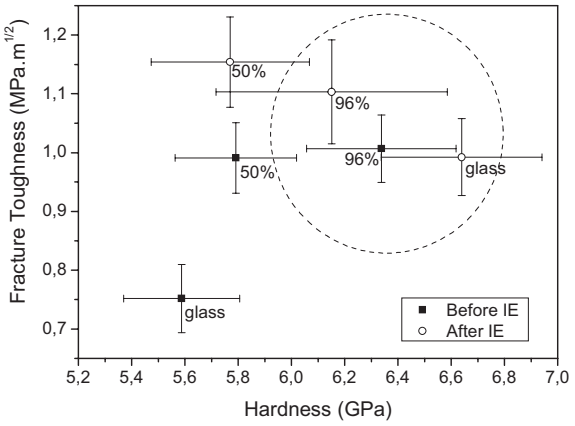

Fig. 8. Plot of Indentation fracture toughness as a function of hardness for all samples investigated. The glass-ceramics inside the dashed circle showed the best ballistic impact resistance for the conditions of the present experiments.

tration by the projectile occurred for the others samples at impact energy as low as 0.5 J, which indicates that there is a limiting value for the material to be useful in ballistic armour applications when it is used on its own (without backing layers). A damage parameter was introduced in order to quantify the extent of macro- and microstructural damage in impacted samples. The present results may be useful for the design of transparent glass-ceramic microstructures for ballistic protection applications.

Experimental

Material: The production of the glass-ceramic included glass melting of raw materials (after powder mixing), and subsequent heat treatment for 4 hrs at a temperature 50 *K* below the glass transition temperature (Tg) in order to remove residual stresses inside the samples. After annealing, all samples were treated using a controlled heat-treatment temperature above Tg. The crystalline fractions studied in the present investigation were (vol. %): 0 % (glass), 50 % and 96 %. The crystalline volume fraction was determined by optical observations using a Leica DMRX light microscope. For each sample at least 40 different areas were analysed, in which the crystals were counted using a grid, and the results averaged. The microstructure exhibited the same morphology composed of cubic shaped crystals. The optical transmittance was measured using a Perkin Elmer UV/Vis/NIR Spectrometer.

The difference in the processing of the glass-ceramics was the time of heat-treatment between 1 and 30 hrs, which led to different crystallinity. Fracture surfaces and polished samples were observed by scanning electron microscopy (SEM) in order to verify the morphology and size of crystals. The ion exchange toughening (IET) treatment was realized for 8 hrs at 460 °C using KNO_3.

Mechanical Tests: Samples in the form of cylindrical bars of nominal dimensions 40 mm in length and 4.5 mm in diameter were used. An optical polished surface was attained. The Young's modulus was measured using the impulse excitation technique (Mk5 Grindsonic®, J. W. Lemmens Ltd., Leuven, Belgium). Hardness and indentation fracture toughness (IFT) were measured by the Vickers indentation method.[37,38] A micro hardness tester (Zwick/ Roell Indentec ZHV, Ulm, Germany) was used, Loads of 1 N were applied for 10 s. Vickers indents, used to induce cracks for indentation fracture toughness measurements, were made using the same device. A minimum of 20 indentations was measured for each sample. For each indent, measurements of the relevant characteristic lengths were made (either indent diagonals or crack lengths). Only symmetrical indentations were used. IFT values were calculated using the expression formulated by Niihara.[38] This equation was chosen due to recent results obtained by Vullo et al,[41] who discovered that this formula better correlates with values obtained by the more rigorous Chevron Notch Test. Niihara's equation can be written as:[38]

$$K_{IC} = 0.035 \left(\frac{l}{a}\right)^{-\frac{1}{2}} \left(\frac{H}{E\Phi}\right)^{-\frac{2}{5}} \left(\frac{H\sqrt{a}}{\Phi}\right) \quad (2)$$

Where K_{Ic} is the IFT, a is the diagonal length of the indentation, l is the crack length, H is the Vickers hardness value, E is Young's modulus, and F is a constant approximately = 3.

Crack propagation in different samples was observed by low magnification optical microscopy.

Ballistic tests: Ballistic tests were carried out by impacting glass and glass-ceramic samples with projectiles fired with a laboratory gas gun. The cylindrical samples were 40 mm in diameter and 4.5 mm in thickness, they were optically polished on both sides. The projectiles were glass beads and steel balls measuring 8 mm and 5 mm in diameter, respectively, and weighting 0.167 g and 0.897 g, respectively. The projectile velocities during this investigation were approximately 80 m/s and 150 m/s. Although the velocities are much lower than those usually employed in testing materials for ballistic resistance applications, we have left the term "ballistic" to refer to our tests in order to be in agreement with the related literature.[7,13] Projectile velocities were determined using a timing device, which contains a light source and measures the time between the shadows due to the projectile flight. The samples were clamped to a steel sample holder. The gun employed for this study was a single stage laboratory gas gun capable of firing spherical projectiles. A detailed description of the facility used is given in the literature.[7] The gun uses compressed nitrogen gas to fire the projectile and is operated by a bursting-diaphragm firing mechanism which controls the velocity. The compressed gas is transferred from the cylinder to the gas reservoir, which is joined to a breech adaptor. A suitable diaphragm is placed between the barrel and the breech adaptor. The pressure in the reservoir causes the diaphragm to rupture, shooting the projectile through the barrel. The velocity of the projectile is controlled by the pressure, which is required to burst the diaphragm. The macroscopic damage (cracking) of the samples after impacts was recorded using a digital camera. It was also confirmed that after ballistic testing the glass projectiles disintegrated for all conditions investigated.

Received: September 17, 2006
Final version: November 03, 2006

[1] S. R. Choi, J. M. Pereira, L. A. Janosik, R. T. Bhatt, *Mater. Sci. Eng. A* **2004**, *379*, 411.
[2] J. Persson, K. Breder, D. J. Rowcliffe, *J. Mater. Sci.* **1993**, *28*, 6484.
[3] C. G. Knight, M. V. Swain, M. M. Chaudhri, *J. Mater. Sci.* **1977**, *12*, 1573.
[4] L. R. Dharani, J. Wei, J. Yu, J. E. Minor, R. A. Behr, P. A. Kremer, *Glass Res. Ceram. Bull.* **2005**, 42.
[5] P. V. Grant, W. J. Cantwell, *J. Testing Eval. JTEVA*, **1999**, *27*, 177.
[6] M. Flinders, D. Ray, A. Anderson, R. A. Cutler, *J. Am. Ceram. Soc.* **2005**. *88*, 2217.
[7] F. McQuillan, Impact. University of London, *Ph D thesis* **1992**.
[8] M. M. Chaudhri, C. R. Kurkjian, *J. Amer. Ceram. Soc.* **1986**, *69*, 404.
[9] M. M. Chaudhri, S. M. Walley, *Phil. Mag. A*, **1978**, *37*, 153.
[10] M. M. Chaudhri, *J. Mater. Sci.* **1989**, *24*, 3441.
[11] A. Ball, *J. Phys. IV*, **1997**, *7*, 921.
[12] C. Kaufmann, D. Cronin, M. Worswick, G. Pageau, A. Beth, *Shock Vibr.* **2003**, *10* , 51.
[13] A. R. Boccaccini, S. Atiq, D. N. Boccaccini, J. Dlouhy, C. Kaya, *Compos. Sci. Tech.* **2005**, *65*, 325.
[14] E. Strassburger, *Int. J. Appl. Cer. Tech.* **2004**, *1*, 235.
[15] O. Peitl, E. D. Zanotto, *J. Non-Cryst. Solids* **1999**, *247*, 39.
[16] G. J. Liu, H. B. Qiu, R. Todd, R. J. Brooke, J. K. Guo, *Mater. Res. Bull.* **1998**, *33*, 281.
[17] Patents, e.g.: WO200290279-A; WO200290279-A1; US-2003013593-A1; US6632758; EP1170262-A; EP1170262-

A1; US2002022564-A1; CN1333194-A; JP2002154841-A; KR2002003502-A
[18] W. Pannhorst, *Glass Sci. Tech.* **2005**, *75*, 78.
[19] G. H. Beall, D. A. Duke, *J. Mater. Sci.* **1969**, *4*, 340.
[20] B. N. Samson, L. R. Pinckney, J. Wang, G. H. Beall, N. F. Borreli, , *Opt. Lett.* **2002**, *27*, 1309.
[21] G. H. Beall, L. R. Pinckney, *J. Amer. Ceram. Soc.* **1999**, *82*, 5.
[22] L. R. Pinckney, *J. Non-Cryst. Solids*, **1999**, *255*, 171.
[23] W. D. Kingery, H. K. Bowen, D. R. Uhlmann, *Introduction to Ceram.* 2nd Edition, Wiley & Sons New York, London, Sydney, Toronto **1976**.
[24] F. Torres, Y. Benino, T. Komatsu, C. Lavelle, *J. Mater. Sci.* **2001**, *36*, 4961.
[25] S. Hendy, *Appl. Phys. Lett.* **2002**, *81*, 12
[26] M. Mortier, *B-Phys. of Condensed Mater. Stat. Mech. Eletronic Opt. and Magn. Properties*, **2002**, *82*, 745.
[27] F. M. Ernsberger, *Amer. Cer. Soc. Bull.* 1973, *52*, 240.
[28] S. S. Kistler, *J. Amer. Cer. Soc.* **1962**, *45*, 59.
[29] M. E. Nordberg, E. M. Mochel, H. M. Garfinkel, J. S. Olcott, *J. Amer. Cer. Soc.* **1964**, *47*, 215.
[30] A. M. Butaev, *Glass and Ceram.* **1984**, *41*, 62.
[31] H. T. Li, W. D. Fei, D. Z. Yang, *Mater. Sci. Eng.* **2002**, *A33*, 377.
[32] D. J. Green, *J. Non-Cryst. Solids* **2003**, *316*, 35.
[33] J. D. Kuntz, G. D. Zhan, A. K. Mukherjee, *MRS Bull.* **2004**, *29*, 22.
[34] S. Atiq, R. D. Rawlings, A. R. Boccaccini, *Glass Sci. Technol.* **2004**, *1*, 77.
[35] S. D. Stookey, J. S. Olcott, H. M. Garfinkel, D. L. Rothermel, *Adv. in Glass Technol.* Plenum Press, New York **1962**, 397.
[36] T. Berthier, PhD thesis, *Federal Univ. of San Carlos, Dept. Mater. Eng.* San Carlos, Brazil **2006**.
[37] G. R. Anstis, P. Chantikel, B. R. Lawn, D. B. Marshall, *J. Amer. Ceram. Soc.* **1981**, *64*, 533.
[38] K. Niihara, R. Morena, D. P. H. Hasselman, *J. Mater. Sci. Lett.* **1982**, *1*, 13.
[39] W. Höland, G. Beall, *Glass-Ceram. Technol.* Am. Ceram. Soc., Westerville, USA **2002**.
[40] I. Dlouhy, A. R. Boccaccini, *Comp. Tech.* **1996**, *56*, 1415.
[41] P. Vullo, M. J. Davis, *J. Non-Cryst. Solids* **2004**, *349*, 180.

